Research Journal of Applied Sciences, Engineering and Technology 6(6): 1053-1058, 2013
ISSN: 2040-7459; e-ISSN: 2040-7467

Submitted: October 22, 2012 Accepted: December 20, 2012 Published: June 30, 2013

Numerical Simulation of the Submarine Pipeline under Wave Action

Zhi-Yong Zhang and Bing Shi
College of Engineering, Ocean University of China, Qingdao 266100, P.R. China

Abstract: A two-dimensional viscous numerical wave flume is established in this study. The Navier-Stokes equations are discretized by Finite Difference Method (FDM). The turbulence is considered by using the standard *k*-ε turbulence model. Volume of Fluid (VOF) method is adopted to capture the free surface of water wave. A virtual inclined porous structure is devised to absorb the wave energy near the end of computational domain. The numerical wave flume was validated by the comparisons with analytical result. Based on the numerical wave flume, the wave field around submarine pipeline was simulated and the numerical results were compared with experimental data. The comparison results show that the present numerical model works well. The maximum horizontal wave force and vertical wave force increase with the wave height.

Keywords: FDM, porous structure, submarine pipeline, VOF, wave forces

INTRODUCTION

Submarine pipeline which is used to transport oil or gas from ocean platforms to land is one of the most important parts in offshore oil field exploitation system, with the advantages of continuity, convenience, huge capacity and minimal influenced by the weather. Under the influence of waves, the submarine pipeline suffers the variable wave forces and the stability of pipeline will be destroyed in a long time. Thus, it is essential to analyze the submarine pipeline under wave action.

In the study of submarine pipeline under wave action, many scholars carried out the physical model experiments and numerical calculations. (Wang *et al*., 1994) used Finite Difference Method (FDM)-Finite Element Method (FEM) and Large Eddy Simulation (LES) turbulence model to simulate the oscillating flow around the pipeline near a plane. (Li and Chen, 1996) measured the wave forces on a seabed pipeline through physical model experiments. Magda (1997) used a two dimensional FEM to simulate the wave-induced hydrodynamic uplift force acting on a submarine pipeline buried in sandy seabed subjected to the sinusoidal surface waves. Li *et al*. (1999) simulated the flow around the seabed pipeline by using a three-step FEM and LES. Both two-dimensional and three-dimensional numerical simulations were carried out to determine the three-dimensional effect subjected to oscillating flow. Vijaya *et al*. (2005) measured the wave pressure and force caused by random waves on a submarine pipeline. Zang *et al*. (2007) established a numerical wave flume based on finite volume method to simulate the wave field around submarine pipeline.

However, large parts of study on the wave field around submarine pipeline are physical model experiments, which cost much money and time. As for the numerical simulation, the wave condition is often replaced by oscillating flow to ignoring the water surface's change and save computational time, which doesn't agree with the physical truth. In this study a numerical wave flume based on Volume of Fluid (VOF) method and potential flow theory of linear wave is established. This wave flume uses porous structure to absorb wave energy near the outflow boundary. The wave field around submarine pipeline near the sandy bed is analyzed by using this wave flume.

ESTABLISHMENT OF NUMERICAL WAVE FLUME

Governing equations: The basic equations are continuity equation and Navier-Stokes equations. As for the porous media, the basic equations are also the continuity equation Eq. (1) and the modified Navier-Stokes equations Eq. (2-3) (Mohammed *et al*., 2003). For the two-phase model, advection equations of fluid density and viscosity Eq. (4-5) are also used:

$$\frac{\partial(r_x u)}{\partial x}+\frac{\partial(r_z w)}{\partial z}=0 \tag{1}$$

$$\lambda_v\frac{\partial u}{\partial t}+\frac{\partial(\lambda_x u^2)}{\partial x}+\frac{\partial(\lambda_z uw)}{\partial z}=-r_v\frac{\partial \psi}{\partial x}+\frac{\partial}{\partial x}\{r_x\mu_e(2\frac{\partial u}{\partial x})\}+\frac{\partial}{\partial z}\{r_z\mu_e(\frac{\partial u}{\partial z}+\frac{\partial w}{\partial x})\}-R_x \tag{2}$$

$$\lambda_v\frac{\partial w}{\partial t}+\frac{\partial(\lambda_x uw)}{\partial x}+\frac{\partial(\lambda_z w^2)}{\partial z}=-r_v\frac{\partial \psi}{\partial z}+\frac{\partial}{\partial x}\{r_x\mu_e(\frac{\partial w}{\partial x}+\frac{\partial u}{\partial z})\}+\frac{\partial}{\partial z}\{r_z\mu_e(2\frac{\partial w}{\partial z})\}-R_z \tag{3}$$

Corresponding Author: Zhi-Yong Zhang, College of Engineering, Ocean University of China, Qingdao 266100, P.R. China

$$\frac{\partial(r_v\rho)}{\partial t}+\frac{\partial(r_x u\rho)}{\partial x}+\frac{\partial(r_z w\rho)}{\partial z}=0 \quad (4)$$

$$\frac{\partial(r_v\mu)}{\partial t}+\frac{\partial(r_x u\mu)}{\partial x}+\frac{\partial(r_z w\mu)}{\partial z}=0 \quad (5)$$

where, t is time ; x, z are horizontal and vertical coordinates; u, w are horizontal and vertical velocity components; $\psi = p/\rho+gz$; ρ is density of fluid, p is pressure, g is gravitational acceleration; μ_e is kinematic viscosity; r_v is volume porosity; r_x, r_z are superficial porosity components in the x and z projections; R_x, R_z are drag and resistance force exerted by porous media. λ_x, λ_z, λ_v, R_x and R_z are given by:

$$\left.\begin{aligned}\lambda_x &= r_x+(1-r_x)C_M\\ \lambda_z &= r_z+(1-r_z)C_M\\ \lambda_v &= r_v+(1-r_v)C_M\end{aligned}\right\} \quad (6)$$

$$R_x=\frac{1}{2}\frac{C_D}{\Delta x}(1-r_x)u\sqrt{u^2+w^2} \quad (7)$$

$$R_z=\frac{1}{2}\frac{C_D}{\Delta z}(1-r_z)w\sqrt{u^2+w^2} \quad (8)$$

where, C_D and C_M are the drag and inertial coefficients. The values of C_D and C_M depend on the porous material properties and incident wave condition (Karim *et al*., 2009).

Free surface model: VOF method is used to capture the free-surface of fluid. The surface between water and air is captured by solve the equation about volume fraction scalar α (Hirt and Nichols, 1981):

$$\frac{\partial\alpha}{\partial t}+\nabla\cdot(\mathrm{u}\alpha)=0 \quad (9)$$

Here α is the volume fraction for the two fluids defined by:

$$\alpha=\begin{cases}0 & \text{volume occupied air}\\ 1 & \text{volume occupied water}\end{cases} \quad (10)$$

The fractions of water and air have the same velocity field and pressure field. However, the density and viscosity in the turbulence model are given by:

$$\rho=\alpha\rho_w+(1-\alpha)\rho_a \quad (11)$$

$$\mu=\alpha\mu_w+(1-\alpha)\mu_a \quad (12)$$

where, ρ_W and ρ_a are density of water and air respectively. μ_W and μ_a are viscosity of water and air respectively.

Turbulence model: The turbulence model selects the standard k-ε model (Lauder and Spalding, 1973):

$$\mu_t=C_\mu\rho\frac{k^2}{\varepsilon} \quad (13)$$

$$\frac{\partial k}{\partial t}+\nabla\cdot(\mathrm{u}k)=\frac{1}{\rho}\nabla(\frac{\mu_t}{\sigma_k}\nabla k)+2\frac{\mu_t}{\rho}\left|\nabla\mathrm{u}\right|-\varepsilon \quad (14)$$

$$\frac{\partial\varepsilon}{\partial t}+\nabla\cdot(\mathrm{u}\varepsilon)=\frac{1}{\rho}\nabla(\frac{\mu_t}{\sigma_\varepsilon}\nabla\varepsilon)+2\frac{C_1\mu_t}{\rho}\left|\nabla\mathrm{u}\right|^2\frac{\varepsilon}{k}-C_2\frac{\varepsilon^2}{k} \quad (15)$$

where,
μ_t = The eddy viscosity
k = Turbulence kinetic energy
ε = Turbulence energy dissipation rate

The constants C_μ, C_1, C_2, σ_k, σ_ε take the values of 0.09, 1.44, 1.92, 1.0 and 1.3 respectively.

Wave generation: In this study, the wave is generated by describing the inlet velocity boundary condition. According to the potential theory (Dean and Dalrymple, 1991), the linear wave's velocities and wave profile are given by x-direction velocity:

$$u(x,z,t)=\frac{A\omega\cosh[k(z+h)]\cos(-\omega t+\varphi)}{2\sinh(kh)} \quad (16)$$

z-direction velocity:

$$w(x,z,t)=\frac{A\omega\sinh[k(z+h)]\sin(-\omega t+\varphi)}{2\sinh(kh)} \quad (17)$$

Vertical distance from wave surface to static water level:

$$\eta(x,t)=\frac{A}{2}\cos(-\omega t+\varphi) \quad (18)$$

where,
A = The wave height
K = The wave number
H = The static water depth
T = Wave period and wave frequency $\omega = 2\pi/TT$

Wave-absorbed method: As for the numerical wave flume, it is impossible to define a large enough computational domain such that the wave reflection can be ignored. In the limited computational domain, the wave reflection has to be eliminated, for example, the

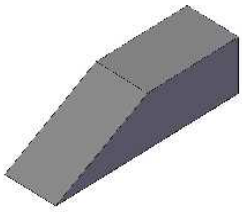

Fig. 1: The schematic of porous structure

methods used by Orlanski (1976), Clément (1996) and Twu *et al*. (2002). In this study, the virtual inclined porous media (Fig. 1) is used to absorb the wave energy near the end of wave flume. The porous media has a slope 1:2, 3 m in length and 0.5 m in height. The porosity is 0.7, which is suitable in this study.

Solution algorithm: The governing equations are discretized using the finite difference method. A fully implicit first-order time-marching scheme is applied. The momentum advection is treated by second-order scheme. The pressure-velocity segregated method involving successive over relaxation iteration method is used to solve the governing equations.

Verification of numerical wave flume: The rectangle flume without pipeline is simulated to verify the numerical wave flume's reliability. The flume is 20 m length as shown in Fig. 2. The region from x = 16 m and x = 19 m is set as porous region. The wave height A is 0.08 m and wave period T is 1.6s. The computational domain is 0.5 m in height and static water depth h = 0.3 m. The whole rectangle flume is discretized by structural grids and the total number of cells is 306920.The grid refinement is used near the water surface in order to track the free surface accurately.

Figure 3 shows the time history of water depth at the inlet boundary. It is observed that the wave profile agrees with the analytical result. Stable water wave is generated. Figure 4 shows the time history of wave elevation at x = 10 m inside the numerical wave flume. It was observed that the present numerical results are generally in good agreement with the analytical result. It is able to produce stable wave trains. It is also found that the wave amplitude of the present numerical result is slightly smaller than that of analytical result. This is due to the viscous and turbulent dissipation

RESULTS AND DISCUSSION

As for the numerical simulation, the pipeline is located at x = 10 m in the numerical wave flume and the simulation cases are shown in Table 1. Besides, the position along the pipeline is defined by angle which is shown in Fig. 5.

Figure 6 shows the wave profiles at five typical instants during one wave period, i.e., t = 0, T/4, T/2, 3T/4 and T. It can be observed that the wave field around submarine pipeline is simulated accurately.

Flow pattern: Under the circumstance of uniform current, the vortex only appear at downstream from pipeline However, in case of wave, the vortexes are observed at both sides of pipeline. The vortex structures are shown in Fig. 7.

Fig. 2: Computational domain

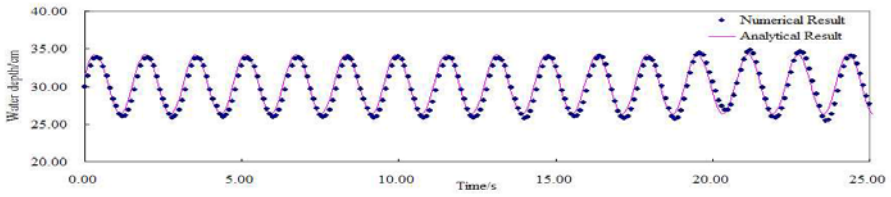

Fig. 3: Time history of water depth at the position x = 0 m

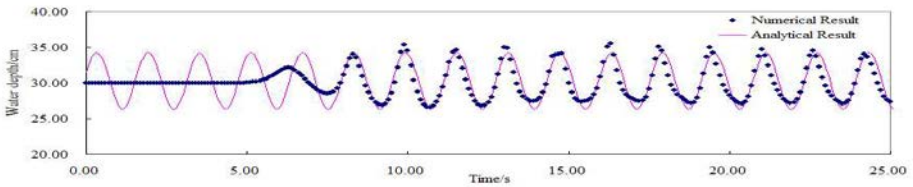

Fig. 4: Time history of water elevation at the position of x = 10 m

Table 1: Simulation cases

Run	Wave height (m)	Wave period (s)	Water depth (m)	Pipeline diameter (m)
1	0.06	1.6	0.30	0.1
2	0.08	1.6	0.30	0.1
3	0.12	1.6	0.30	0.1

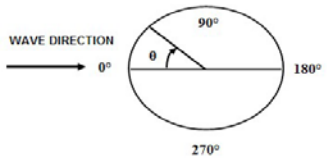

Fig. 5: Layout of the pipeline

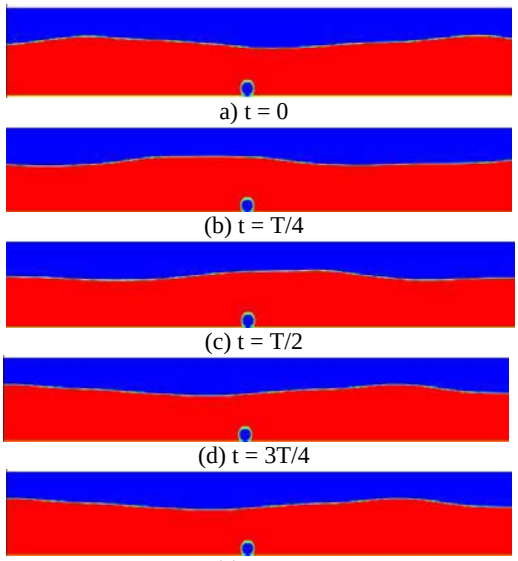

Fig. 6: Motion process of wave, the red region is fluid region

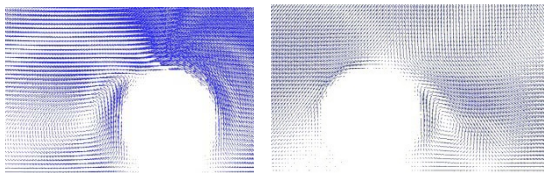

Fig. 7: Fluid field around pipeline

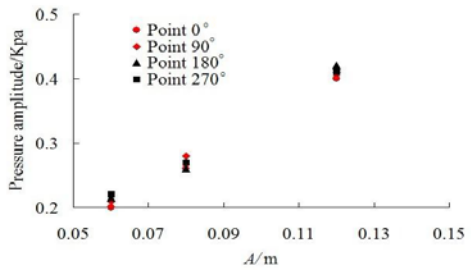

Fig. 8: Variance of average pressure amplitudes with wave height

The vortex appearance at the two sides of pipeline happens at different time. When the wave peak doesn't arrive at the pipeline, the water above the pipeline flow left to make the wave peak move forward. The left region of pipeline is downstream in which the vortex appears. In contrast, when the wave hollow is in front of the pipeline, the water flow right and the right region of pipeline is downstream where the vortex appears. The time gap between the wave peak and wave hollow shows that the vortexes appear in turn at both sides of pipeline each half of wave period. Because the seabed is fixed bed in experiment and simulation, the seabed is not changeable. However, the real condition is generally sand bed which is easier to be scoured. The sands at both sides of pipeline will be rolled up and cause the scour of seabed. Thus the vortex around the pipeline is one of important factors that induce the sediment scour.

Wave pressure: Under the circumstance of current, the pressure difference between upstream and downstream of pipeline is significant. The pressure upstream is larger than pressure downstream. Lu *et al*. (2006), Liang *et al*. (2004) and Zang *et al*. (2007) have investigated the mechanism of pressure difference focusing on the local scour around submarine pipeline by means of CFD model. However, in the case of wave action, the pressure difference and fluctuation are also attributed to the periodical oscillation of velocity field induced by the water waves. Figure 8 shows the average pressure amplitudes at four points in different cases. Since the wave lengths are about 3m, which is much larger than the diameter of pipeline, the phase lag between the two points of 0° and 180° is small. In addition, the ratio of pipeline diameter to wave length is about 0.03, much smaller than 0.2, therefore the wave diffraction can be ignored. The amplitudes of pressures at four points are almost the same in case of the same wave height. In addition, the pressure amplitude increases with the wave height linearly.

Wave forces: The dimensionless wave forces can be expressed as follows:
Horizontal wave force:

$$f_h = F_H / (\rho g h D / 2) \tag{19}$$

Vertical wave force:

$$f_v = F_V / (\rho g h D / 2) \tag{20}$$

where, F_H, F_V are horizontal and vertical wave forces in unit length of pipeline respectively (N/m).

Jothi *et al*. (1985) did many experiments to study the wave forces on submarine pipeline. Figure 9 shows maximum horizontal wave force f_{hmax} and vertical wave

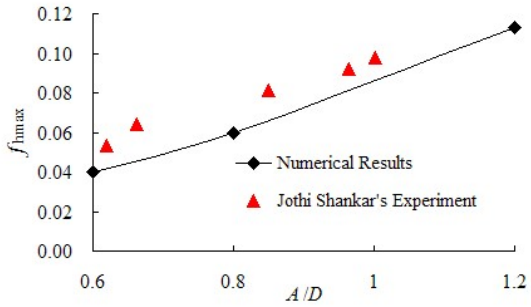

Horizontal wave force

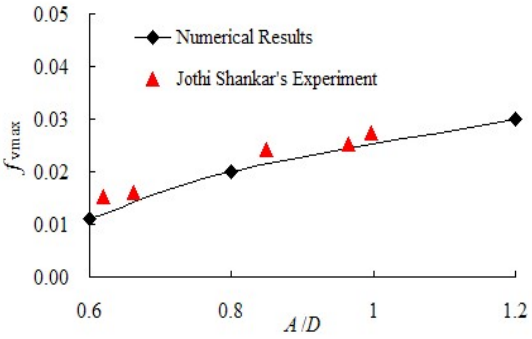

Vertical wave force

Fig. 9: Variance of maximum wave force with relative wave height

force f_{vmax} in different cases. It can be inferred that the numerical results are in agreement with the experimental results. The maximum horizontal and vertical wave force both increase with the relative wave height's increasing.

CONCLUSION

A numerical wave flume was established based on FDM and VOF method .It was used to simulate the wave field around submarine pipeline. The simulation results were compared with those experiment data. The main conclusions are as follows:

- The numerical wave flume based on the finite difference solution of Navier-Stokes equations closed by k-ε turbulent model and the Volume of Fluid method for free surface capture is in good agreement with analytical results. The virtual inclined porous structure can absorb the wave energy effectively.
- The wave field around submarine pipeline under wave action is simulated by the two-dimensional numerical wave flume developed in this study. With the increase of wave height, the maximum wave force increase nearly linearly. Besides, the maximum value of horizontal wave force is larger than maximum value of vertical wave force.

ACKNOWLEDGMENT

This study was financially supported by National Nature Science Fund of China (Grant No. 50879084; 51279189). The writers are grateful for the comments provided by the Editors and the reviewers, which have significantly improved the quality of the study.

REFERENCES

Clément, A., 1996. Coupling of two absorbing boundary conditions for 2D time-domain simulations of free surface gravity waves. J. Comput. Phys., 126: 139-151.

Dean, R.G. and R.A. Dalrymple, 1991. Water Wave Mechanics for Engineers and Scientist. World Scientific, Singapore.

Hirt, C.W. and B.D. Nichols, 1981. Volume of Fluid (VoF) method for the dynamics of free boundaries. J. Comput. Phys., 39: 201-225.

Jothi, S.N., H. Raman and V. Sundar, 1985. Wave forces on large offshore pipelines. Ocean Eng., 12(2): 99-115.

Karim, M.F., K. Tanimoto and P.D. Hieu. 2009. Modelling and simulation of wave transformation in porous structures using VOF based two-phase flow model. Appl. Math. Modell., 33(1): 343-360.

Lauder, B. and D. Spalding, 1973. The numerical computation of turbulent flows. Comput. Method Appl. Mech. Eng., 13(2): 269-289.

Li, Y. and B. Chen, 1996. Physical model test of pipelines under wave action. Marine Sci. Bull., 15(5): 68-73.

Li, Y., B. Chen and G. Lai, 1999. The numerical simulation of wave forces on seabed pipeline by three-step finite element method and large eddy simulation. Acta Oceanol. Sinica, 21(6): 87-93.

Liang, D.F., L. Cheng and F. Li, 2004. Numerical modelling of scour below a pipeline in currents. Part I: Flow simulation. Coastal Eng., 52(1): 25-42.

Magda, W., 1997. Wave-induced uplift force on a submarine pipeline buried in a compressible seabed. Ocean Eng., 24(6): 551-576.

Mohammed, F.K., T. Katsutoshi and D.H. Phung, 2003. Simulation of wave transformation in vertical permeable structure. Proceedings of the 13th International Offshore and Polar Engineering Conference. Honolulu, Hawaii, USA.

Orlanski, I., 1976. A simple boundary condition for unbounded hyperbolic flows. J. Comput. Phys., 21(3): 251-269.

Twu, S., C. Liu and C. Twu, 2002. Wave damping characteristics of vertically stratified porous structures under oblique wave action. Ocean Eng., 29(11): 1295-1311.

Vijaya, K.A., S. Neelamani and S.N. Rao, 2005. Wave interaction with a submarine pipeline in clayey soil due to random waves. Ocean Eng., 32(13): 1517-1538.

Wang, G., G. Lai and Y. Li, 1994. FDM-FEM approach for numerical simulation of a circular cylinder in oscillatory plus mean flow coming from arbitrary directions. J. Hydrodynamic., 9(4): 224-233.

Zang, Z.P., B. Teng, W. Bai and C. Liang, 2007. A finite volume solution of wave forces on submarine pipelines. Ocean Eng., 34(4): 1955-1964.